Journal of Sound and Vibration (2001) **241**(5), 735–754
doi:10.1006/jsvi.2000.3316, available online at http://www.idealibrary.com on IDEAL®

WAVE PROPAGATION, REFLECTION AND TRANSMISSION IN TUNABLE FLUID-FILLED BEAMS

N. R. HARLAND, B. R. MACE† AND R. W. JONES‡

Department of Mechanical Engineering, The University of Auckland, Private Bag 92019, *Auckland, New Zealand. E-mail: brm@isvr.soton.ac.uk*

(*Received* 21 *March* 2000)

This paper concerns wave motion in tunable fluid-filled beams. The beams comprise two elastic faceplates with a central core of tunable fluid such as electro-rheological or magneto-rheological fluid. Free wave propagation is considered and three wave modes are seen to exist. The corresponding wavenumbers depend on the viscoelastic properties of the tunable fluid, which in turn depend on the field applied to the fluid. Consequently, the wavenumbers can be controlled. A systematic technique for describing wave transmission and reflection in one-dimensional waveguides is described. This involves transformations between wave amplitudes and waveguide displacements and internal forces. Expressions are derived which describe wave reflection at a boundary, reflection and transmission at a change in section and reflection and transmission at an attachment. Numerical results are presented for electro-rheological fluid-filled beams and the junction between such a beam and an Euler–Bernoulli beam. The reflection and transmission coefficients also depend on the applied field so that the transmission characteristics are tunable.

1. INTRODUCTION

A tunable fluid-filled beam is a composite beam which comprises elastic faceplates between which is sandwiched a layer of tunable fluid. Typical examples of such fluids are electro-rheological (ER) and magneto-rheological (MR) fluids. If no yield takes place, then these fluids behave like viscoelastic materials whose properties (the shear and loss moduli) vary, depending on the strength of the electric or magnetic field to which they are exposed.

Dynamically, a tunable fluid-filled beam behaves in the same manner as a composite beam whose central core is some viscoelastic material [1]. Such beams have been used to add damping to structures. Their vibration characteristics are, however, fixed at the time of manufacture. Replacing the central core with a tunable fluid raises the possibility of tuning the passive vibration characteristics of the beam by changing the field to which the tunable fluid is exposed.

Tunable fluid-filled beams have been the subject of many recent publications (e.g., references [2–10]). In these, the vibrational behaviour was modelled using modal methods. In this paper, however, a wave approach is adopted. Expressions describing the propagation, reflection and transmission of waves are developed. The ultimate aim is to be able to adaptively control the transmission or absorption of vibration energy in structures

†Present address: Institute of Sound and Vibration Research, University of Southampton, Highfield, Southampton SO17, 1BJ, U.K.
‡Present address: Department of Computer Science and Electrical Engineering, Luleå University of Technology, SE-97187 Luleå, Sweden.

0022-460X/01/150735 + 20 $35.00/0

by appropriately tuning a part of the structure comprising a tunable fluid-filled beam (see Harland *et al.* [2]).

The next section concerns free wave propagation. The tunable fluid-filled beam is described by the model of Mead *et al.* [1]. Three wave modes exist, the wavenumbers depending on the applied field. Then a general method is described by which waveguide displacements and internal forces can be related to positive- and negative-going wave amplitudes. The method is then used to determine reflection and transmission coefficients at boundaries, junctions between two waveguides with different sections and point attachments. Numerical examples are presented for ER fluid-filled beams and for junctions between Euler–Bernoulli beams and an ER fluid-filled beam.

2. TUNABLE FLUIDS AND BEAMS

In this paper, tunable fluids are defined to be fluids whose properties, in particular the viscoelastic properties, are able to be changed. The ability to change the properties of these fluids is the primary mechanism that will be exploited to create beams whose vibration characteristics can be tuned. The two most common tunable fluids are ER and MR fluids, whose shear properties change in response to an electric field $\mathscr{E}$ and a magnetic field $\mathscr{H}$ respectively.

Generally, ER fluids are suspensions of micron-sized dielectric particles (typical diameters are in the 5–50 μm range) in an insulating fluid, that exhibit changing rheological properties in the presence of an applied electric field. When an electric field of the order 0·1–5·0 kV/mm (AC or DC depending on the fluid) is applied to the fluid, long ordered chains of dielectric particles form between the electrodes. The change in rheology of the fluid occurs within a few milliseconds. Physically, the fluid changes from a viscous oil to an almost solid gel. In MR fluids, the suspensions of micron-sized particles are usually some form of soft-magnetic material and the applied field is magnetic. In general, the viscoelastic characteristics of ER fluids are considerably weaker and less tunable than those of MR fluids (see Weiss *et al.* [11]).

The pre-yield viscoelastic characteristics of a tunable fluid can in general be modelled for vibrational analysis by [3]

$$G = A_0 + A_1 \mathscr{F}^B, \qquad G' = C_0 + C_1 \mathscr{F}^D, \tag{1}$$

where G is the shear modulus and G' the loss modulus of the fluid, A_0, A_1, B, C_0, C_1 and D are constants and $\mathscr{F}$ is the applied field.

2.1. TUNABLE FLUID-FILLED BEAMS

The tunable fluid-filled beams in this paper comprise a layer of tunable fluid sandwiched between two solid elastic layers (see Figure 1). Physical properties of the beam can be changed by tuning the viscoelastic properties of the tunable fluid. The beam can form one component of a larger structure.

Most previous vibrations-related research concerns structures that incorporate ER fluids, rather than MR fluids and all analyses proceed along modal lines. Ghandi *et al.* [4], Coulter *et al.* [5], Choi *et al.* [6] all studied cantilevered ER fluid-filled beams. Significant changes in the natural frequencies of the beams occur in response to an applied electric field. Control methods based on a modal description are then developed to tune the applied field to minimize vibrations at the tip for discrete frequency excitation.

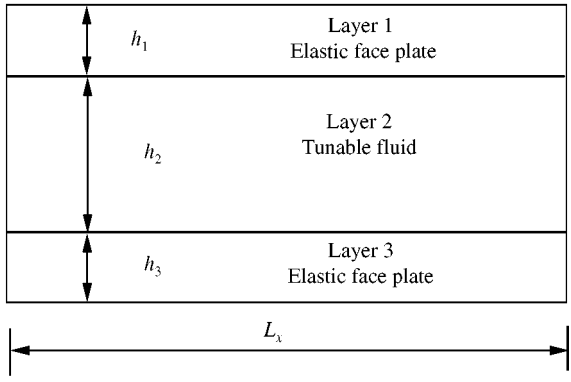

Figure 1. Tunable fluid-filled beam.

Haiqing *et al.* [7] considered a cantilever beam with an ER fluid patch acting as a spring of variable stiffness midway along its length. It was concluded that the beam was more sensitive to changes in the applied electric field than a cantilevered beam completely filled with ER fluid. Don [8] conducted experimental investigations into the vibrations of ER adaptive beam-like and plate-like structures with various boundary conditions. The model of Mead *et al.* [1] was used to predict the response. Oyadiji [9] experimentally studied the dependence of the vibrational response on the area of an ER fluid patch. He concluded that the area covered has a larger effect than varying the electric field applied to the fluid.

Yalcintas [3] developed models to describe ER beams with various boundary conditions and with different electric fields being applied to different regions of the beam. The model of Mead *et al.* [1] was used here also and was seen to be applicable to a number of different beam configurations. Theoretical results were validated by experiment. Neural network models were also developed to control the ER beam. Finally, Lee [10] modelled ER beams with various boundary conditions using a finite element approach.

3. TUNABLE FLUID-FILLED BEAM MODEL

A number of configurations exist for beams filled with tunable fluids. The particular configuration used in this paper is the three-layer sandwich beam shown in Figure 1. In this section, a model of this beam is presented following the work of Mead *et al.* [1] which concerns three-layer sandwich beams with a viscoelastic core. In this paper, the shear properties of the tunable fluid are given by equations (1). This pre-yield assumption was shown to be valid for ER beams by Yalcintas [3]. In her work, she showed that the maximum strain experienced in ER fluid-filled beams is of the order of 10^{-4}, whereas the yield strain was approximately 10^{-3}.

Consider a composite beam comprising two elastic outer layers between which is sandwiched a layer of viscoelastic material or tunable fluid (see Figure 2). The elastic face plates are of thicknesses h_1 and h_3. The viscoelastic layer is of thickness h_2. All layers are of equal width L_y and have length L_x.

The same assumptions as Mead *et al.* [1] are made concerning the material properties and the deformation of the beam. The elastic outer layers are undamped, isotropic and have Young's moduli E_1 and E_3. These layers experience no shear deformation normal to the beam surface. The viscoelastic layer carries shear but no direct stress and has a shear modulus G_2 and a loss factor β. Longitudinal and rotary inertia is neglected in all of the

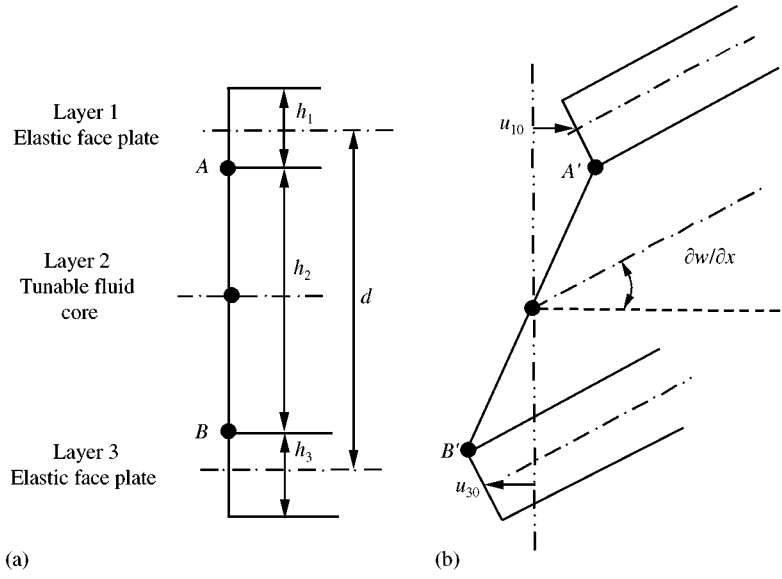

Figure 2. Cross-section of a tunable fluid-filled beam (a) before and (b) after deformation.

layers and the densities of each layer are given by ρ_1, ρ_2 and ρ_3. The whole sandwich beam is assumed to be in pure bending and hence the overall longitudinal force on the beam section is zero. No slip is assumed to occur at the interfaces of the viscoelastic core and elastic layers. All points on a normal to the beam move with the same transverse displacement w. The longitudinal displacement of the midpoints of the elastic layers are given by u_{10} and u_{30} (see Figure 2). Henceforth, it is assumed that the outer layers are identical, so that $h_1 = h_3$, etc.

If a distributed load $p(x, t)$ acts on the beam then [1]

$$\frac{\partial^6 w}{\partial x^6} - g(1+Y)\frac{\partial^4 w}{\partial x^4} + \frac{\bar{m}}{\overline{EI}}\left(\frac{\partial^4 w}{\partial x^2\,\partial t^2} - g\frac{\partial^2 w}{\partial t^2}\right) = \frac{1}{\overline{EI}}\left(\frac{\partial^2 p(x,t)}{\partial x^2} - gp(x,t)\right),$$

$$\overline{EI} = \tfrac{1}{12}L_y(E_1 h_1^3 + E_3 h_3^3),$$

$$\bar{m} = L_y(\rho_1 h_1 + \rho_2 h_2 + \rho_3 h_3),$$

$$g = \frac{G_2^*}{h_2}\left(\frac{1}{E_1 h_1} + \frac{1}{E_3 h_3}\right),$$

$$G_2^* = G_2 + \mathrm{i}G_2',$$

$$Y = \frac{\mathrm{d}^2 L_y}{\overline{EI}}\left(\frac{1}{E_1 h_1} + \frac{1}{E_3 h_3}\right)^{-1},$$

$$d = h_2 + \tfrac{1}{2}(h_1 + h_3), \tag{2}$$

where $\overline{EI}$, $\bar{m}$, g and Y are the total bending stiffness of the beam, the mass per unit length, the shear parameter and the geometric parameter respectively.

The longitudinal displacements are given by

$$u_{10} = \frac{\overline{EI}}{E_1 h_1 \, \mathrm{d}L_y}\left(\frac{1}{g^2}\frac{\partial^5 w}{\partial x^5} - \frac{Y}{g}\frac{\partial^3 w}{\partial x^3} + \frac{1}{g^2}\frac{\bar{m}}{\overline{EI}}\frac{\partial^3 w}{\partial x\,\partial t^2} - Y\frac{\partial w}{\partial x} - \frac{1}{g^2\overline{EI}}\frac{\partial}{\partial x}(p(x,t))\right) \tag{3}$$

and

$$u_{30} = -\frac{E_1 h_1}{E_3 h_3} u_{10}. \tag{4}$$

The net shear force on the section is

$$Q = \frac{\overline{EI}}{g}\frac{\partial}{\partial x}\left(\frac{\partial^4 w}{\partial x^4} - g(1+Y)\frac{\partial^2 w}{\partial x^2} - \frac{p(x,t)}{\overline{EI}} + \frac{\bar{m}}{\overline{EI}}\frac{\partial^2 w}{\partial t^2}\right), \tag{5}$$

while the bending moment

$$M = \frac{\overline{EI}}{g}\left(-\frac{\partial^4 w}{\partial x^4} + g(1+Y)\frac{\partial^2 w}{\partial x^2} + \frac{p(x,t)}{\overline{EI}} - \frac{\bar{m}}{\overline{EI}}\frac{\partial^2 w}{\partial t^2}\right). \tag{6}$$

The axial forces experienced by the top and bottom elastic layers, N_1 and N_3, are given by

$$N_1 = -N_3 = \frac{\overline{EI}}{gd}\left(\frac{\partial^4 w}{\partial x^4} - gY\frac{\partial^2 w}{\partial x^2} - \frac{p(x,t)}{\overline{EI}} + \frac{\bar{m}}{\overline{EI}}\frac{\partial^2 w}{\partial t^2}\right). \tag{7}$$

3.1. WAVE PROPAGATION IN TUNABLE FLUID-FILLED BEAMS

Consider the free vibration problem. A displacement of the form

$$w(x,t) = a\mathrm{e}^{\mathrm{i}(\omega t - kx)} \tag{8}$$

is assumed.

Consequently, the dispersion equation is given by

$$-k^6 - g(1+Y)k^4 + \frac{\bar{m}}{\overline{EI}}k^2\omega^2 + g\frac{\bar{m}}{\overline{EI}}\omega^2 = 0. \tag{9}$$

Equation (9) is cubic in k^2 and thus three pairs of positive- and negative-going waves exist, with wavenumbers k_j, $j = 1, 2, 3$ which are in general complex. In general, the motion is a superposition of all the wave components so that the displacement, for example, can be written as

$$w(x,t) = \sum_{j=1,3}(a_j^+ \mathrm{e}^{-\mathrm{i}k_j x} + a_j^- \mathrm{e}^{+\mathrm{i}k_j x})\mathrm{e}^{\mathrm{i}\omega t}, \tag{10}$$

where a_j^+ and a_j^- are the amplitudes of the positive- and negative-going components of the jth wave mode.

From equation (9) it follows that

$$\omega = \sqrt{\frac{\overline{EI}}{\bar{m}}}\left(\frac{k^6 + g(1+Y)k^4}{k^2 + g}\right)^{1/2} \tag{11}$$

and hence the phase and group velocities are

$$c_p = \sqrt{\frac{\overline{\overline{EI}}}{\bar{m}}} \left(\frac{k^4 + g(1+Y)k^2}{k^2 + g} \right)^{1/2} \tag{12}$$

and

$$c_g = c_p \left(2 - k^2 \left(\frac{1}{k^2 + g} - \frac{1}{k^2 + g(1+Y)} \right) \right) \tag{13}$$

respectively. Note that since Y is positive then the group speed is always less than twice the phase speed.

3.2. NUMERICAL EXAMPLE

Consider an ER fluid-filled beam with aluminium elastic layers and unit width. The properties of the beam are given in Table 1. The shear properties of the ER fluid are taken from Don [8].

Figure 3 shows the real and imaginary parts of the wavenumber for positive travelling waves at $\omega = 10$ rad/s, as functions of applied electric field. Results at other frequencies ($\omega < 1000$ rad/s) are qualitatively similar. The wavenumbers are complex. The real and imaginary parts are related to the phase and attenuation of the wave with distance.

There are three wave modes. For small electric fields wave mode 1 propagates freely with large phase change and attenuates relatively gradually. It can transport energy relatively freely over large distances. Wave mode 2, on the other hand, behaves like a bending near field, having a relatively large imaginary part and a small real part. It thus attenuates rapidly with distance and generally propagates little energy. Wave mode 3 behaves like a "push–pull" axial wave motion in the outer layers. Like wave mode 2, it has small phase changes and attenuates rapidly with distance. At higher fields wave 1 continues to propagate freely but it now has somewhat less attenuation. Wave modes 2 and 3 continue to have small phase changes but both attenuate more rapidly.

Assuming a displacement of unit magnitude (i.e., $|w| = 1$), then the slope w' for each wave mode is shown in Figure 4. The corresponding shear force is shown in Figure 5. Both figures show a dependence on the applied field.

Both rotation and axial motion determine the shear within the viscoelastic layer and consequently the deformation that the ER beam experiences. Typical features of the deformed shape of the cross-section at high and low electric field strengths are shown in Figure 6. At low field strengths the deformations caused by wave modes 1 and 2 are dominated by w' and the beam deforms under these wave types as if the face plates are bending independently with the same displacement and slope. These wave modes are thus analogous to the propagating and nearfield bending wave modes that exist in Euler–Bernoulli beams. On the other hand, the core strain of wave mode 3 is dominated by u_{10} and represents a deformation where a large shearing action occurs in the viscoelastic layer.

TABLE 1

Properties of the ER fluid-filled beam

$h_1 = h_3$ (m)	$\rho_1 = \rho_3$ (kg/m^3)	$E_1 = E_3$ (N/m^2)	h_2 (m)	ρ_2 (kg/m^3)	G_2 (N/m^2)	G_2' (N/m^2)
10^{-3}	$2{\cdot}7 \times 10^3$	$7{\cdot}27 \times 10^{10}$	3×10^{-3}	$1{\cdot}06 \times 10^3$	$5 \times 10^4 \mathscr{E}^2$	$4340 \mathscr{E}^{0{\cdot}35}$

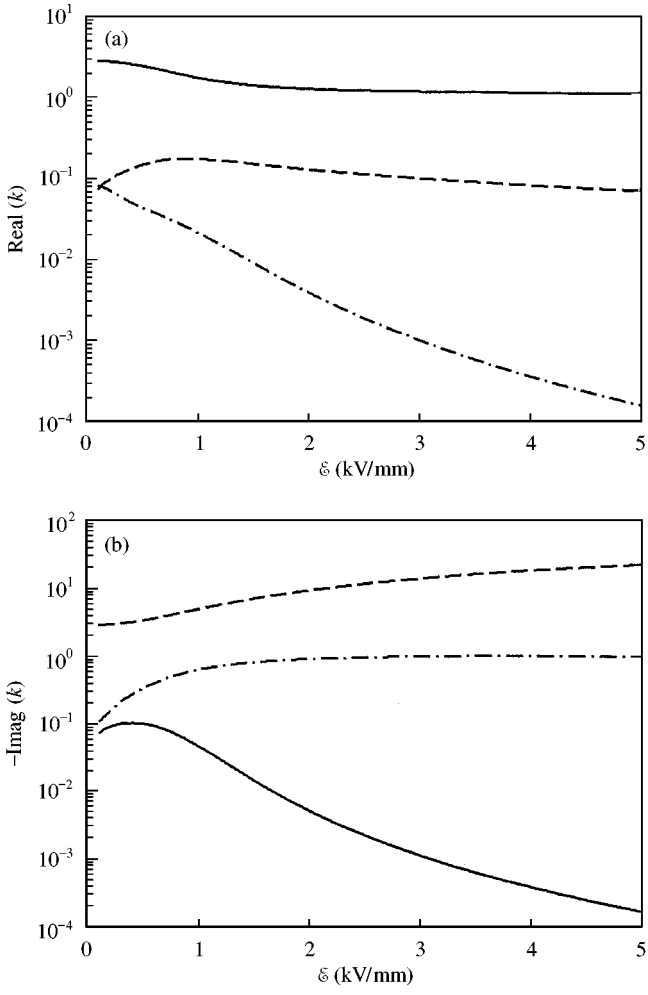

Figure 3. (a) Real and (b) imaginary parts of wavenumbers, $\omega = 10$: ———, wave mode 1; – –, wave mode 2; – · –, wave mode 3.

As the field increases, however, there is a change in the deformed shape of each wave mode. In wave modes 1 and 2 the core strain is spread more evenly between w' and u_{10} and the beam deforms more as a single plane surface. In wave mode 3 the core strain is again spread more evenly but, because w' and u_{10} are out of phase by 180°, the core strain is larger than that experienced by the other wave types. These changes in behaviour with electric field are due to the stiffening of the fluid layer. With a low field the viscoelastic properties of the ER fluid are weak and therefore the fluid transmits little shear stress to the face plates and consequently contributes little to the motion of the beam. With a higher field the fluid is considerably stiffer and thus the transmitted shear stress affects the deformation.

The changes in the behaviour exhibited by each wave mode are also seen in the change in the phase and group speeds. The phase speeds for each wave mode type are shown (see Figure 7). We see that as the electric field increases then phase speeds of wave modes 1 and 2 vary little with the applied electric field. Conversely, the phase speed of wave mode 3 increases rapidly. Relative to wave mode 1, wave modes 2 and 3 propagate little energy.

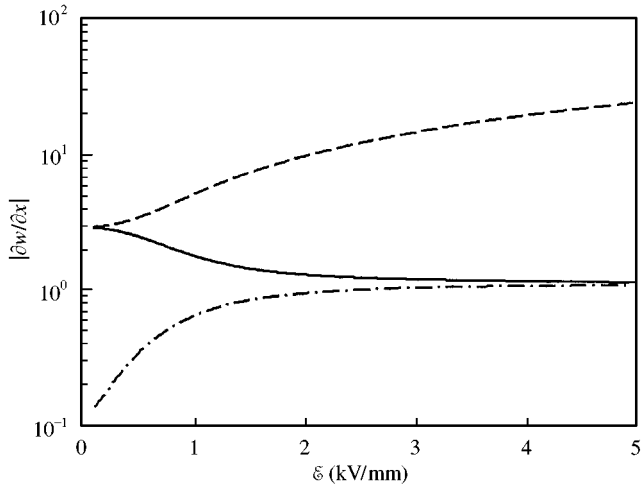

Figure 4. Magnitude of rotation per unit translation, $\omega = 10$: ——, wave mode 1; – –, wave mode 2; –·–, wave mode 3.

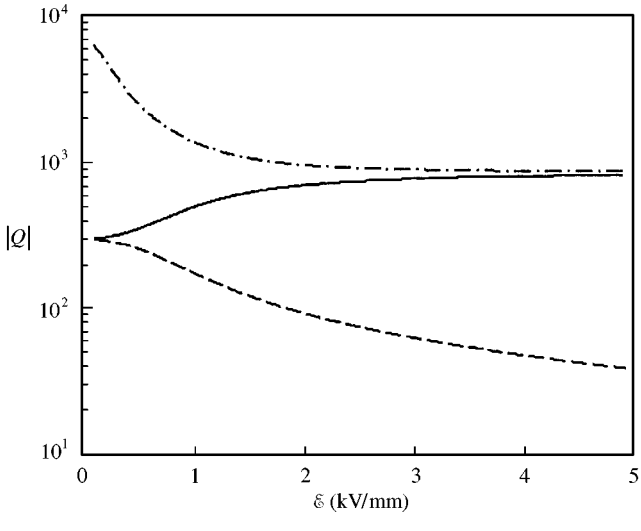

Figure 5. Magnitude of shear force per unit translation, $\omega = 10$: ——, wave mode 1; – –, wave mode 2; –·–, wave mode 3.

4. GENERALIZED WAVES AND THE STATE OF A WAVEGUIDE SECTION

In general, a number of different wave modes may exist in a waveguide. In this section, a general, systematic approach is described which enables the wave amplitudes to be related to the displacements and internal forces in the waveguide. Later this approach is adopted to determine reflection and transmission coefficients at boundaries, discontinuities and junctions between beams.

4.1. WAVE AMPLITUDE VECTORS

It is convenient to group the amplitudes of the waves at a cross-section of a waveguide into vectors of positive and negative going waves. For a waveguide carrying n different wave

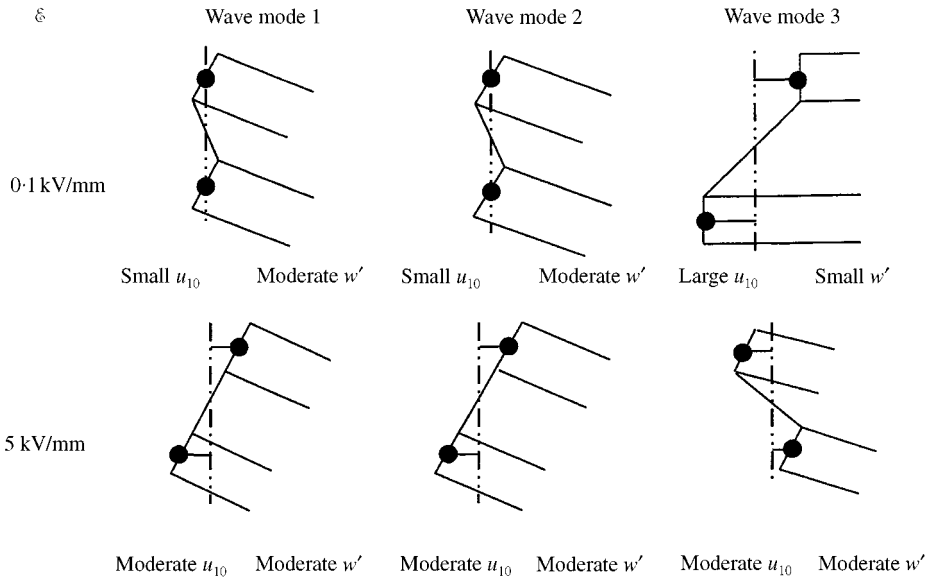

Figure 6. Characteristics of deformation of tunable fluid-filled beam for each wave mode, $\omega = 10$.

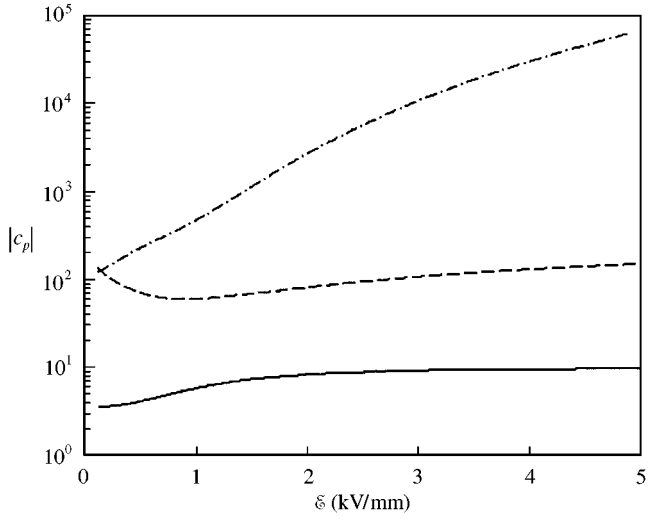

Figure 7. Phase speed, $\omega = 10$: ———, wave mode 1; – –, wave mode 2; – · –, wave mode 3.

types the amplitudes of the positive and the negative travelling waves $\mathbf{a}^+$ and $\mathbf{a}^-$ at a cross-section can be written as

$$\mathbf{a}^+ = \begin{Bmatrix} a_1^+ \\ a_2^+ \\ \vdots \\ a_n^+ \end{Bmatrix}, \qquad \mathbf{a}^- = \begin{Bmatrix} a_1^- \\ a_2^- \\ \vdots \\ a_n^- \end{Bmatrix}. \tag{14}$$

Specifically, the wave amplitude vectors for Euler–Bernoulli beams and are given by

$$\mathbf{a}^+ = \begin{Bmatrix} a_P^+ \\ a_N^+ \end{Bmatrix}, \qquad \mathbf{a}^- = \begin{Bmatrix} a_P^- \\ a_N^- \end{Bmatrix}, \tag{15}$$

where $a_P^\pm$ and $a_N^\pm$ represent the amplitudes of the propagating and nearfield waves while for tunable fluid-filled beams

$$\mathbf{a}^+ = \begin{Bmatrix} a_1^+ \\ a_2^+ \\ a_3^+ \end{Bmatrix}, \qquad \mathbf{a}^- = \begin{Bmatrix} a_1^- \\ a_2^- \\ a_3^- \end{Bmatrix}. \tag{16}$$

4.2. STATE OF A SECTION IN TERMS OF WAVE COMPONENTS

It is possible to write expressions for the displacements and internal forces at a cross-section of a waveguide, using the wave amplitude vectors described in the previous section. As an example consider an Euler–Bernoulli beam. Suppressing time dependence, then the displacement of a cross-section can be written as

$$w = [1\ 1]\,\mathbf{a}^+ + [1\ 1]\,\mathbf{a}^-, \tag{17}$$

while the slope is given by

$$\frac{\partial w}{\partial x} = [-\mathrm{i}k\ \ -k]\,\mathbf{a}^+ + [\mathrm{i}k\ k]\,\mathbf{a}^-. \tag{18}$$

Similarly, the shear force and bending moment are given by

$$Q = EI[-\mathrm{i}k^3\ k^3]\,\mathbf{a}^+ + EI[\mathrm{i}k^3\ \ -k^3]\,\mathbf{a}^-, \tag{19}$$

$$M = EI[-k^2\ k^2]\,\mathbf{a}^+ + EI[-k^2\ k^2]\,\mathbf{a}^-. \tag{20}$$

As a second example, consider tunable fluid-filled beams. The three degrees of freedom of the cross-section are related to the vectors of wave amplitudes by

$$\begin{Bmatrix} w \\ \partial w/\partial x \\ u_{10} \end{Bmatrix} = \begin{bmatrix} 1 & 1 & 1 \\ -\mathrm{i}k_1 & -\mathrm{i}k_2 & -\mathrm{i}k_3 \\ \tilde{u}_{10}(k_1) & \tilde{u}_{10}(k_2) & \tilde{u}_{10}(k_3) \end{bmatrix} \mathbf{a}^+ + \begin{bmatrix} 1 & 1 & 1 \\ \mathrm{i}k_1 & \mathrm{i}k_2 & \mathrm{i}k_3 \\ -\tilde{u}_{10}(k_1) & -\tilde{u}_{10}(k_2) & -\tilde{u}_{10}(k_3) \end{bmatrix} \mathbf{a}^-, \tag{21}$$

where

$$\tilde{u}_{10}(k_j) = \frac{\overline{EI}}{E_1 h_1\, \mathrm{d}L_y} \frac{1}{g^2} \left(-\mathrm{i}(k_j)^5 - \mathrm{i}gY(k_j)^3 + \left(\omega^2 \frac{\bar{m}}{\overline{EI}} + g^2 Y \right) k_j \right) \tag{22}$$

is the axial deformation per unit wave amplitude produced by the jth wave type.

Similarly, the corresponding internal forces are given by

$$\begin{Bmatrix} Q \\ M \\ N_1 \end{Bmatrix} = \begin{bmatrix} \tilde{Q}(k_1) & \tilde{Q}(k_2)1 & \tilde{Q}(k_3) \\ \tilde{M}(k_1) & \tilde{M}(k_2) & \tilde{M}(k_3) \\ \tilde{N}_1(k_1) & \tilde{N}_1(k_2) & \tilde{N}_1(k_3) \end{bmatrix} \mathbf{a}^+ + \begin{bmatrix} -\tilde{Q}(k_1) & -\tilde{Q}(k_2) & -\tilde{Q}(k_3) \\ \tilde{M}(k_1) & \tilde{M}(k_2) & \tilde{M}(k_3) \\ \tilde{N}_1(k_1) & \tilde{N}_1(k_2) & \tilde{N}_1(k_3) \end{bmatrix} \mathbf{a}^-, \tag{23}$$

where

$$\tilde{Q}(k_j) = \frac{\overline{EI}}{g}\left(-\mathrm{i}(k_j)^5 - g(1 + Y)\mathrm{i}(k_j)^3 + \frac{\bar{m}}{\overline{EI}}\omega^2 \mathrm{i}(k_j)\right), \tag{24}$$

$$\tilde{M}(k_j) = \frac{\overline{EI}}{g}\left(-(k_j)^4 - g(1 + Y)(k_j)^2 + \frac{\bar{m}}{\overline{EI}}\omega^2 \right) \tag{25}$$

and

$$\tilde{N}_1(k_j) = \frac{\overline{EI}}{gd}\left((k_j)^4 + gY(k_j)^2 - \frac{\bar{m}}{\overline{EI}}\omega^2 \right). \tag{26}$$

4.3. DISPLACEMENT AND INTERNAL FORCE VECTORS

The degrees of freedom of the cross-section and the corresponding generalized internal forces describe the state of the cross-section at any point and can be related to the wave amplitudes straightforwardly. It is convenient to group the displacements into a vector, termed the *displacement vector*, **W**. Similarly, the internal forces and moments can be grouped into the *internal force vector*, **F**. Corresponding entries in **W** and **F** give a generalized displacement and its corresponding generalized force.

For an Euler–Bernoulli beam

$$\mathbf{W} = \begin{Bmatrix} w \\ \partial w/\partial x \end{Bmatrix} \tag{27}$$

and

$$\mathbf{F} = \begin{Bmatrix} Q \\ M \end{Bmatrix}. \tag{28}$$

For a tunable fluid-filled beam the displacement and internal force vectors are given by equations (21) and (23).

Let us define Ψ^+ and Ψ^- as *displacement matrices* for waves travelling in the positive and negative x directions, respectively, such that

$$\mathbf{W} = \Psi^+\mathbf{a}^+ + \Psi^-\mathbf{a}^-. \tag{29}$$

In a similar way, Φ^+ and Φ^- are defined as *internal force matrices* for waves travelling in the positive and negative x directions, respectively, so that

$$\mathbf{F} = \Phi^+\mathbf{a}^+ + \Phi^-\mathbf{a}^-. \tag{30}$$

The positive- and negative-going displacement matrices are related to each other such that

$$\Psi^- = \psi\Psi^+, \tag{31}$$

where ψ is a diagonal matrix whose elements are ± 1, relating the phases of the positive- and negative-going wave components.

Similarly, the positive- and negative-going internal force matrices are related by

$$\Phi^- = \phi\Phi^+, \tag{32}$$

where

$$\phi = -\psi. \tag{33}$$

For an Euler–Bernoulli beam these matrices are given by

$$\Psi^+ = \begin{bmatrix} 1 & 1 \\ -\mathrm{i}k & -k \end{bmatrix}, \qquad \Psi^- = \begin{bmatrix} 1 & 1 \\ \mathrm{i}k & k \end{bmatrix}, \qquad \psi = \begin{bmatrix} 1 & 0 \\ 0 & -1 \end{bmatrix} \tag{34}$$

and

$$\Phi^+ = \begin{bmatrix} -\mathrm{i}EIk^3 & EIk^3 \\ -EIk^2 & EIk^2 \end{bmatrix}, \qquad \Phi^- = \begin{bmatrix} \mathrm{i}EIk^3 & -EIk^3 \\ -EIk^2 & EIk^2 \end{bmatrix}, \qquad \phi = \begin{bmatrix} -1 & 0 \\ 0 & 1 \end{bmatrix}, \tag{35}$$

while for tunable fluid-filled beams the matrices are given by equations (21), (23) and

$$\psi = \begin{bmatrix} 1 & 0 & 0 \\ 0 & -1 & 0 \\ 0 & 0 & -1 \end{bmatrix}, \qquad \phi = \begin{bmatrix} -1 & 0 & 0 \\ 0 & 1 & 0 \\ 0 & 0 & 1 \end{bmatrix}. \tag{36}$$

The displacement and internal force matrices indicate the contribution that wave components travelling in a particular direction make to the waveguide deformations and internal forces.

4.4. TIME-AVERAGED ENERGY FLOW

The time-averaged energy flow Π in a cross-section is given in terms of the displacement and internal force vectors by

$$\Pi = -\tfrac{1}{2}\,\mathrm{Re}\{\mathrm{i}\omega \mathbf{W}^H \mathbf{F}\}. \tag{37}$$

where H is the Hermitian operator. Substituting for the displacement and internal force vectors from equations (34) and (35) gives

$$\Pi = -\tfrac{1}{2}\omega\,\mathrm{Im}\{\mathbf{a}^{+H}\Psi^{+H}\Phi^{+}\mathbf{a}^{+} + \mathbf{a}^{-H}\Psi^{-H}\Phi^{-}\mathbf{a}^{-} + \mathbf{a}^{-H}\Psi^{-H}\Phi^{+}\mathbf{a}^{+} + \mathbf{a}^{+H}\Psi^{+H}\Phi^{-}\mathbf{a}^{-}\}. \tag{38}$$

The time-averaged energy flow has four components. The first two arise from the waves travelling in either the positive or the negative x directions, while the other two terms arise from the interaction of these waves.

5. WAVE REFLECTION AND TRANSMISSION

Generally, beams are used to form members of a larger structure. Beams are finite in length, have boundaries and may have discontinuities along their length. If a wave in a beam is incident upon a boundary then it is reflected and if it is incident upon a discontinuity then it will be reflected and transmitted. In general, an incident wave of a particular wave mode is scattered into all wave modes that the particular waveguide can carry. The amplitudes of the reflected and transmitted waves are given by reflection and transmission matrices. These matrices are determined for a particular discontinuity by the particular discontinuity and equilibrium equations applicable for that discontinuity. This section concerns the reflection and transmission of waves at various boundaries and discontinuities.

5.1. BEAM BOUNDARIES

Suppose waves $\mathbf{a}^+$ are incident upon a boundary of a waveguide as shown in Figure 8. They give rise to reflected waves $\mathbf{a}^-$. Equilibrium equations can always be written such that

$$\mathbf{AF} + \mathbf{BW} = \mathbf{0}, \tag{39}$$

where $\mathbf{A}$ and $\mathbf{B}$ are matrices whose elements may involve stiffness, damping, etc. and are in general complex and frequency dependent. In terms of the incident waves the reflected waves are given by

$$\mathbf{a}^- = \mathbf{r}^{aa}\mathbf{a}^+. \tag{40}$$

It then follows that

$$\mathbf{r}^{aa} = -(\mathbf{A}\Phi^- + \mathbf{B}\Psi^-)^{-1}(\mathbf{A}\Phi^+ + \mathbf{B}\Psi^+) \tag{41}$$

is the reflection matrix that gives the amplitudes of the reflected waves in terms of those of the incident waves. The superscript indicates that waves in waveguide a are reflected into waves in waveguide a. Unless $\mathbf{r}^{aa}$ is a diagonal matrix then wave mode conversion occurs, in that an incident wave of one type will be scattered into waves of all types.

Consider the case of a waveguide with a free end. Since the end is free then the vector of internal forces is zero. Consequently,

$$\mathbf{A} = \mathbf{I}, \qquad \mathbf{B} = \mathbf{0}, \tag{42}$$

where $\mathbf{I}$ and $\mathbf{0}$ are the identity and the null matrices respectively. The reflection matrix is therefore given by

$$\mathbf{r}_F^{aa} = -(\Phi^-)^{-1}\Phi^+. \tag{43}$$

Similarly, if the boundary is clamped then the displacement vector is zero and therefore

$$\mathbf{A} = \mathbf{0}, \qquad \mathbf{B} = \mathbf{I} \tag{44}$$

and hence the reflection matrix is given by

$$\mathbf{r}_C^{aa} = (\Psi^-)^{-1}\Psi^+. \tag{45}$$

In a similar way, reflection coefficients can be found for end conditions that have attachments such as springs, dampers, masses and dynamic absorbers.

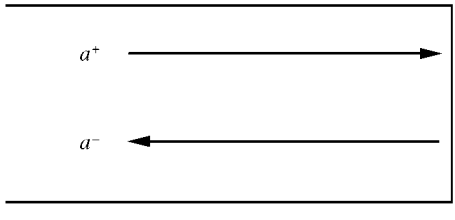

Figure 8. Wave reflection from a boundary.

5.1.1. *Reflections from tunable fluid-filled beam boundaries*

Consider the reflection of waves from a boundary of a tunable fluid-filled beam. The reflection matrices for free and clamped boundaries of these beams are given by equations (43) and (45) respectively. For a simply supported boundary the beam is physically constrained so that $w = M = 0$. Since the beam is free to rotate N_1 is also zero. Therefore, in this case,

$$\mathbf{A} = \begin{bmatrix} 0 & 0 & 0 \\ 0 & 1 & 0 \\ 0 & 0 & 1 \end{bmatrix}, \qquad \mathbf{B} = \begin{bmatrix} 1 & 0 & 0 \\ 0 & 0 & 0 \\ 0 & 0 & 0 \end{bmatrix}. \tag{46}$$

The reflection matrix is given by

$$\mathbf{r}_S^{aa} = -\begin{bmatrix} 1 & 1 & 1 \\ \tilde{M}(-k_1) & \tilde{M}(-k_2) & \tilde{M}(-k_3) \\ \tilde{N}_1(-k_1) & \tilde{N}_2(-k_2) & \tilde{N}_3(-k_3) \end{bmatrix}^{-1} \begin{bmatrix} 1 & 1 & 1 \\ \tilde{M}(k_1) & \tilde{M}(k_2) & \tilde{M}(k_3) \\ \tilde{N}_1(k_1) & \tilde{N}_2(k_2) & \tilde{N}_3(k_3) \end{bmatrix}, \tag{47}$$

which reduces to

$$\mathbf{r}_S^{aa} = -\mathbf{I}. \tag{48}$$

Note as is the case with Euler–Bernoulli beams wave mode conversion does not occur since $\mathbf{r}_S^{aa}$ is diagonal. Note that this reflection matrix holds for Euler–Bernoulli beams. The only difference is, however, that the identity matrix for Euler–Bernoulli beams is 2×2 as opposed to the 3×3 size for fluid-filled beams.

5.1.2. *Numerical example*

As an example, consider wave reflection from a free end of the ER fluid-filled beam described in section 3. Figure 9 shows various components of the reflection matrix $\mathbf{r}_F^{aa}$ for an incident mode 3 wave at $\omega = 10$ as a function of the applied electric field. Note that the reflection coefficients depend upon the electric field. Consequently, an applied electric field can be used to alter the wave reflection characteristics in ER fluid-filled beams. Similar variations in structural parameters can be achieved in tunable structural elements in general.

5.2. JUNCTIONS BETWEEN BEAMS

When waveguides form part of a structure it is not uncommon for them to experience discontinuities along their length. These discontinuities can include attachments such as springs, dampers, etc., a change in section and so on. If a wave is incident upon any discontinuity then it will be scattered, being partly reflected and partly transmitted. In general, wave mode conversion occurs, in that an incident wave of one mode will be scattered into waves of all modes. This is equally true when a wave is incident upon a junction between waveguides of different types.

Consider the junction j between two waveguides, a and b (see Figure 10). The number of wave modes in beams a and b are n_a and n_b; n_a does not necessarily equal n_b. Incident waves of amplitude $\mathbf{a}_j^+$ and $\mathbf{b}_j^-$ at the junction are scattered into waves $\mathbf{a}_j^-$ and $\mathbf{b}_j^+$.

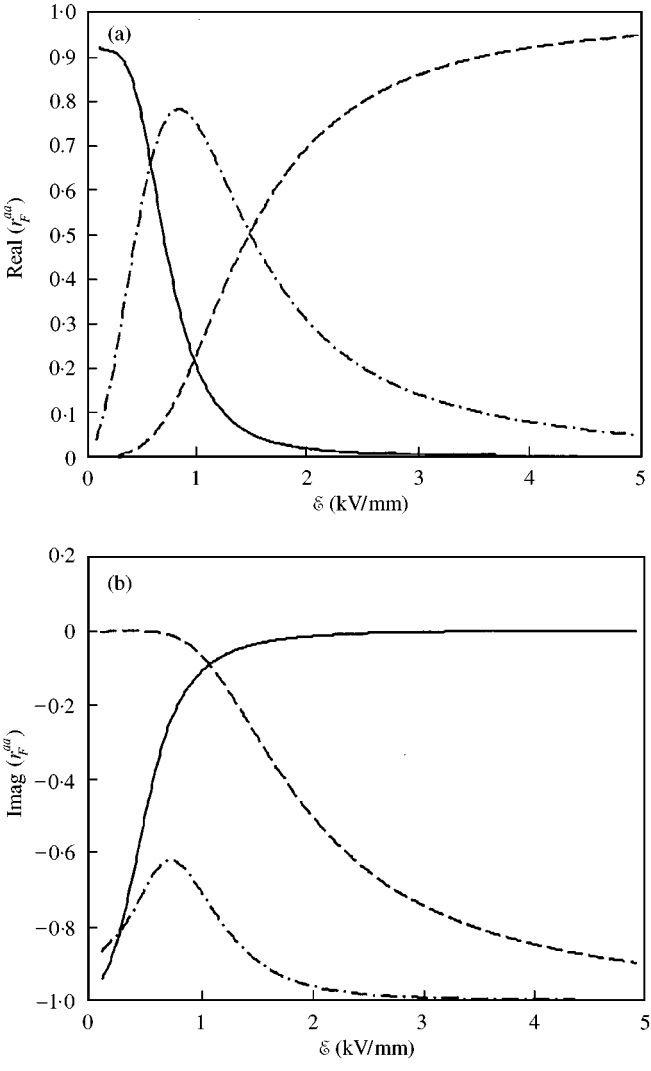

Figure 9. (a) Real part and (b) imaginary part of the reflection coefficients for a wave mode 3 wave incident upon a free boundary, $\omega = 10$: ———, $r_F^{aa}(k_1)$; – –, $r_F^{aa}(k_2)$; – · –, $r_F^{aa}(k_3)$.

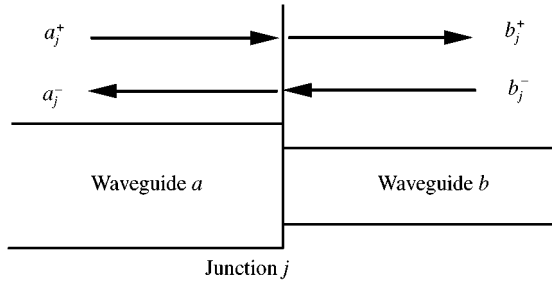

Figure 10. Waves at a junction j.

At the junction, the displacement vector for waveguide a is given by

$$\mathbf{W}_a = \Psi_a^+ \mathbf{a}_j^+ + \Psi_a^- \mathbf{a}_j^- \tag{49}$$

and the internal force vector is given by

$$\mathbf{F}_a = \Phi_a^+ \mathbf{a}_j^+ + \Phi_a^- \mathbf{a}_j^- \tag{50}$$

with similar expression holding for beam b.

Since waveguides a and b are physically connected then there are continuity and equilibrium relations at the junction. These are given by

$$\mathbf{C}_a \mathbf{W}_a = \mathbf{C}_b \mathbf{W}_b \tag{51}$$

and

$$\mathbf{E}_a \mathbf{F}_a = \mathbf{E}_b \mathbf{F}_b, \tag{52}$$

respectively, where $\mathbf{C}_{a,b}$ are continuity matrices and $\mathbf{E}_{a,b}$ are equilibrium matrices.

Equations (49) and (50) and the continuity and equilibrium equations (51) and (52), give

$$\begin{bmatrix} -\mathbf{C}_a \Psi_a^- & \mathbf{C}_b \Psi_b^+ \\ -\mathbf{E}_a \Phi_a^- & \mathbf{E}_b \Phi_b^+ \end{bmatrix} \begin{Bmatrix} \mathbf{a}_j^- \\ \mathbf{b}_j^+ \end{Bmatrix} = \begin{bmatrix} \mathbf{C}_a \Psi_a^+ & -\mathbf{C}_b \Psi_b^- \\ \mathbf{E}_a \Phi_a^+ & -\mathbf{E}_b \Phi_b^- \end{bmatrix} \begin{Bmatrix} \mathbf{a}_j^+ \\ \mathbf{b}_j^- \end{Bmatrix}. \tag{53}$$

Assuming that the matrix on the left-hand side is invertible then

$$\begin{Bmatrix} \mathbf{a}_j^- \\ \mathbf{b}_j^+ \end{Bmatrix} = \begin{bmatrix} -\mathbf{C}_a \Psi_a^- & \mathbf{C}_b \Psi_b^+ \\ -\mathbf{E}_a \Phi_a^- & \mathbf{E}_b \Phi_b^+ \end{bmatrix}^{-1} \begin{bmatrix} \mathbf{C}_a \Psi_a^+ & -\mathbf{C}_b \Psi_b^- \\ \mathbf{E}_a \Phi_a^+ & -\mathbf{E}_b \Phi_b^- \end{bmatrix} \begin{Bmatrix} \mathbf{a}_j^+ \\ \mathbf{b}_j^- \end{Bmatrix}. \tag{54}$$

Note that equation (54) is in the form

$$\begin{Bmatrix} \mathbf{a}_j^- \\ \mathbf{b}_j^+ \end{Bmatrix} = \mathbf{T} \begin{Bmatrix} \mathbf{a}_j^+ \\ \mathbf{b}_j^- \end{Bmatrix}, \tag{55}$$

where $\mathbf{T}$ is the *scattering matrix* given by

$$\mathbf{T} = \begin{bmatrix} \mathbf{r}_j^{aa} & \mathbf{t}_j^{ba} \\ \mathbf{t}_j^{ab} & \mathbf{r}_j^{bb} \end{bmatrix}, \tag{56}$$

where $\mathbf{r}$ and $\mathbf{t}$ are *reflection* and *transmission matrices*, respectively, the superscripts identifying the waveguides of the incoming and outgoing waves respectively.

If $n_a \leqslant n_b$ then by simplifying equation (54) using its partitioned matrix inverse and then comparing the result to equation (56), the reflection and transmission matrices are found to be given by

$$\begin{aligned}
\mathbf{r}_j^{aa} &= (-\mathbf{E}_a \Phi_a^- + \mathbf{E}_b \Phi_b^+ (\mathbf{C}_b \Psi_b^+)^{-1} \mathbf{C}_a \Psi_a^-)^{-1} (\mathbf{E}_a \Phi_a^+ - \mathbf{E}_b \Phi_b^+ (\mathbf{C}_b \Psi_b^+)^{-1} \mathbf{C}_a \Psi_a^+), \\
\mathbf{t}_j^{ab} &= (\mathbf{C}_b \Psi_b^+)^{-1} (\mathbf{C}_a \Psi_a^+ + \mathbf{C}_a \Psi_a^- \mathbf{r}_j^{aa}), \\
\mathbf{t}_j^{ba} &= (\mathbf{E}_a \Phi_a^- - \mathbf{E}_b \Phi_b^+ (\mathbf{C}_b \Psi_b^+)^{-1} \mathbf{C}_a \Psi_a^-)^{-1} (\mathbf{E}_b \Phi_b^- - \mathbf{E}_b \Phi_b^+ (\mathbf{C}_b \Psi_b^+)^{-1} \mathbf{C}_b \Psi_b^-), \\
\mathbf{r}_j^{bb} &= (\mathbf{C}_b \Psi_b^+)^{-1} (-\mathbf{C}_b \Psi_b^- + \mathbf{C}_a \Psi_a^- \mathbf{t}_j^{ba}).
\end{aligned} \tag{57}$$

If $n_b \geqslant n_a$, similar equations hold with the sub- and superscripts a and b reversed.

5.2.1. *Junction between an Euler–Bernoulli beam and a tunable fluid-filled beam*

As an example, consider the junction between an Euler–Bernoulli beam a and a tunable fluid-filled beam b. From continuity at the junction, the slopes, displacements and the axial deformation on both sides of the junction must equal each other. As a consequence, the continuity matrices are given by

$$\mathbf{C}_a = \begin{bmatrix} 1 & 0 \\ 0 & 1 \\ 0 & \frac{1}{2}d \end{bmatrix}, \qquad \mathbf{C}_b = \begin{bmatrix} 1 & 0 & 0 \\ 0 & 1 & 0 \\ 0 & 0 & 1 \end{bmatrix}. \tag{58}$$

From equilibrium the shear forces and the bending moments on both sides of the junction must also equal each other while the net axial force is zero. Hence,

$$\mathbf{E}_a = \begin{bmatrix} 1 & 0 \\ 0 & 1 \end{bmatrix}, \qquad \mathbf{E}_b = \begin{bmatrix} 1 & 0 & 0 \\ 0 & 1 & 0 \end{bmatrix}. \tag{59}$$

5.2.2. *Numerical example*

Consider the junction between an Euler–Bernoulli beam and an ER fluid-filled beam. In this example, the Euler–Bernoulli beam is made of aluminium. It is assumed to be of unit width with its remaining properties given in Table 2. The ER fluid-filled beam is described in section 3.4.

Figures 11 and 12 show the reflection and transmission coefficients for an incident propagating wave in the Euler–Bernoulli beam. Note that the incident wave is scattered into all three modes in the ER fluid-filled beam (although the amplitude of the mode 2 wave is small) as well as being reflected into both propagating waves and near fields in the Euler–Bernoulli beam. From Figure 11 it is seen that about half of the incident energy is reflected and that a relatively small reflected near field is produced.

Note also that it is possible to tune the fluid properties to achieve desired reflection and transmission characteristics. As an example, applying an electric field of 1·366 kV/mm causes a reflected propagating wave of minimum amplitude.

5.3. LOCALIZED ATTACHMENTS

As a final case, consider reflection and transmission at a junction where a spring, mass, damper, etc. has been attached to a junction between two waveguides a and b. In this situation, the continuity equation is given by equation (51) while the equilibrium equation is given by

$$\mathbf{F}_b - \mathbf{F}_a = \mathbf{K}\mathbf{W}_a, \tag{60}$$

TABLE 2

Material and geometric properties of the Euler–Bernoulli beam

h	E	ρ
5×10^{-3}	$7{\cdot}27 \times 10^{10}$	$2{\cdot}7 \times 10^{3}$

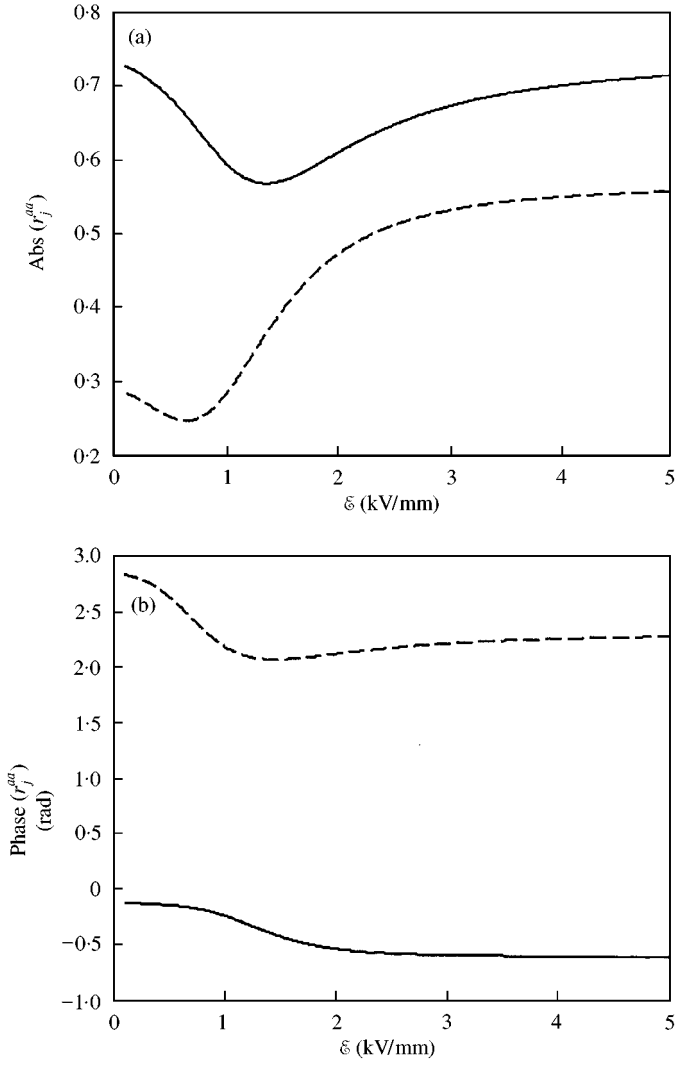

Figure 11. (a) Magnitude and (b) phase of the reflection matrix coefficients for a propagating wave incident upon a junction between an Euler–Bernoulli and an ER fluid-filled beam, $\omega = 10$: ——, propagating; – –, near field.

where **K** is a dynamic stiffness matrix that may be complex and frequency dependent, depending on the type of attachments.

In this situation, the reflection and transmission matrices of the discontinuity are given by

$$\mathbf{r}_j^{aa} = (-\mathbf{K}\Psi_a^- - \mathbf{E}_a\Phi_a^- + \mathbf{E}_b\Phi_b^+(\mathbf{C}_b\Psi_b^+)^{-1}\mathbf{C}_a\Psi_a^-)^{-1}(\mathbf{K}\Psi_a^+ + \mathbf{E}_a\Phi_a^+ - \mathbf{E}_b\Phi_b^+(\mathbf{C}_b\Psi_b^+)^{-1}\mathbf{C}_a\Psi_a^+),$$

$$\mathbf{t}_j^{ab} = (\mathbf{C}_b\Psi_b^+)^{-1}(\mathbf{C}_a\Psi_a^+ + \mathbf{C}_a\Psi_a^-\mathbf{r}_j^{aa}),$$

$$\mathbf{t}_j^{ba} = (\mathbf{K}\Psi_a^- + \mathbf{E}_a\Phi_a^- - \mathbf{E}_b\Phi_b^+(\mathbf{C}_b\Psi_b^+)^{-1}\mathbf{C}_a\Psi_a^-)^{-1}(\mathbf{E}_b\Phi_b^- - \mathbf{E}_b\Phi_b^+(\mathbf{C}_b\Psi_b^+)^{-1}\mathbf{C}_b\Psi_b^-),$$

$$\mathbf{r}_j^{bb} = (\mathbf{C}_b\Psi_b^+)^{-1}(-\mathbf{C}_b\Psi_b^- + \mathbf{C}_a\Psi_a^-\mathbf{t}_j^{ba}). \tag{61}$$

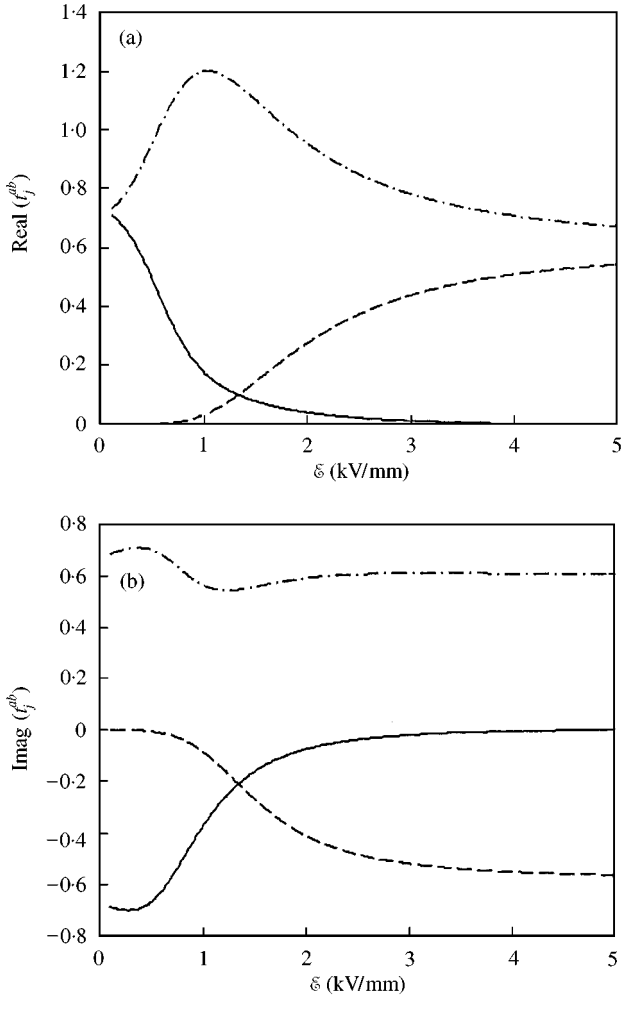

Figure 12. (a) Real part and (b) imaginary part of the transmission matrix coefficients for a propagating wave incident upon a junction between an Euler–Bernoulli and an ER fluid-filled beam, $\omega = 10$: ——, $t_j^{ab}(k_1)$; – –, $t_j^{ab}(k_2)$; – · –, $t_j^{ab}(k_3)$.

When there is no junction and the waveguide is uniform (i.e., waveguides a and b are identical) then

$$\mathbf{r}_j^{aa} = -(\mathbf{K}\Psi_a^- + 2\Phi_a^-)^{-1}\mathbf{K}\Psi_a^+ = \psi(\mathbf{t}_j^{ba} - \mathbf{I}) = \mathbf{r}_j^{bb},$$

$$\mathbf{t}_j^{ab} = \mathbf{I} + \psi\mathbf{r}_j^{aa} = (\mathbf{K}\Psi_a^- + 2\Phi_a^-)^{-1}2\Phi_a^- = \mathbf{t}_j^{ba}. \tag{62}$$

It can be shown that a junction with localized attachments can be modelled as two discontinuities separated by zero distance, one discontinuity being a uniform waveguide with localized attachments, the other being a junction without attachments. The order of the discontinuities does not matter. The resulting net reflection and net transmission matrices are the same as those given by equations (57).

6. CONCLUSIONS

This paper considered wave motion in tunable fluid-filled beams. Expressions for the wavenumbers and the reflection and transmission coefficients were derived, the latter using a matrix method which is applicable to wave analysis in general one-dimensional waveguides. Numerical results were presented for an ER fluid-filled beam and for the junction between an Euler–Bernoulli beam and an ER fluid-filled beam.

The important feature that distinguishes this structural element from more traditional passive components is that the characteristics of the wave motion, i.e., the wavenumbers, and reflection and transmission coefficients, are tunable to an extent by varying the electric or magnetic field to which the tunable fluid is exposed. In a subsequent paper [2], this behaviour is exploited by incorporating a tunable beam within a larger structure, the aim being to tune the vibrational behaviour of the structure as a whole.

ACKNOWLEDGMENTS

The authors would like to acknowledge the assistance of the New Zealand Returned Services Association, the Levin Returned Services Association, Heritage Manawatu and Heritage New Zealand.

REFERENCES

1. D. J. MEAD and S. MARKUS 1969 *Journal of Sound and Vibration* **10**, 163–175. The forced vibration of a three-layer, damped sandwich beam with arbitrary boundary conditions.
2. B. R. MACE, R. W. JONES and N. R. HARLAND 2000 *Journal of the Acoustical Society of America*. Wave transmission through structural inserts. (to appear)
3. M. YALCINTAS 1995 *PhD Thesis, Lehigh University, U.S.A.* An analytical and experimental investigation of electro-rheological material based adaptive structures.
4. M. V. GANDHI, B. S. THOMPSON and S.-B. CHOI 1989 *Journal of Composite Materials* **23**, 1232–1255. A new generation of innovative ultra advanced intelligent composite materials featuring electro-rheological fluids: an experimental investigation.
5. J. P. COULTER and T. G. DUCLOS 1989 in *Proceedings of the Second International Conference on ER Fluids* (J. D. Carlson, editor) 300–325. Applications of electro-rheological materials in vibration control.
6. Y. D. CHOI, A. F. SPRECHER and H. CONRAD 1990 *Journal of Intelligent Material Systems and Structures* **1**, 91–104. Vibration characteristics of a composite beam containing an electro-rheological fluid.
7. G. HAIQING and L. M. KING 1996 *Journal of Intelligent Material System and Structures* **7**, 89–96. Experimental investigations on tension and compression properties of an electro-rheological material.
8. D. L. DON 1993 *Master of Science Thesis, Lehigh University, U.S.A.* An investigation of electro-rheological material adaptive structures.
9. S. O. OYADUI 1996 *Journal of Intelligent Material Systems and Structures* **7**, 541–549. Applications of electro-rheological fluids for constrained layer treatments of structures.
10. C.-Y. LEE 1995 *Journal of Intelligent Material Systems and Structures* **6**, 718–728. Finite element formulation of a sandwich beam with embedded electro-rheological fluids.
11. K. D. WEISS, J. D. CARLSON and D. A. NIXON 1994 *Journal of Intelligent Material Systems and Structures* **5**, 772–775. Viscoelastic properties of magneto- and electro-rheological fluids.